

BRAIN COMMUNICATIONS

Interictal magnetoencephalography abnormalities to guide intracranial electrode implantation and predict surgical outcome

Thomas W. Owen,¹ Vytene Janiukstyte,¹ Gerard R. Hall,¹ Fahmida A. Chowdhury,^{2,3} Beate Diehl,^{2,3} Andrew McEvoy,^{2,3} Anna Misericchi,^{2,3} Jane de Tisi,^{2,3,4}  John S. Duncan,^{2,3,4} Fergus Rugg-Gunn,^{2,3} Yujang Wang^{1,2,3,5} and  Peter N. Taylor^{1,2,3,5}

Intracranial EEG is the gold standard technique for epileptogenic zone localization but requires a preconceived hypothesis of the location of the epileptogenic tissue. This placement is guided by qualitative interpretations of seizure semiology, MRI, EEG and other imaging modalities, such as magnetoencephalography. Quantitative abnormality mapping using magnetoencephalography has recently been shown to have potential clinical value. We hypothesized that if quantifiable magnetoencephalography abnormalities were sampled by intracranial EEG, then patients' post-resection seizure outcome may be better. Thirty-two individuals with refractory neocortical epilepsy underwent magnetoencephalography and subsequent intracranial EEG recordings as part of presurgical evaluation. Eyes-closed resting-state interictal magnetoencephalography band power abnormality maps were derived from 70 healthy controls as a normative baseline. Magnetoencephalography abnormality maps were compared to intracranial EEG electrode implantation, with the spatial overlap of intracranial EEG electrode placement and cerebral magnetoencephalography abnormalities recorded. Finally, we assessed if the implantation of electrodes in abnormal tissue and subsequent resection of the strongest abnormalities determined by magnetoencephalography and intracranial EEG corresponded to surgical success. We used the area under the receiver operating characteristic curve as a measure of effect size. Intracranial electrodes were implanted in brain tissue with the most abnormal magnetoencephalography findings—in individuals that were seizure-free postoperatively ($T = 3.9$, $P = 0.001$) but not in those who did not become seizure-free. The overlap between magnetoencephalography abnormalities and electrode placement distinguished surgical outcome groups moderately well (area under the receiver operating characteristic curve = 0.68). In isolation, the resection of the strongest abnormalities as defined by magnetoencephalography and intracranial EEG separated surgical outcome groups well, area under the receiver operating characteristic curve = 0.71 and area under the receiver operating characteristic curve = 0.74, respectively. A model incorporating all three features separated surgical outcome groups best (area under the receiver operating characteristic curve = 0.80). Intracranial EEG is a key tool to delineate the epileptogenic zone and help render individuals seizure-free postoperatively. We showed that data-driven abnormality maps derived from resting-state magnetoencephalography recordings demonstrate clinical value and may help guide electrode placement in individuals with neocortical epilepsy. Additionally, our predictive model of postoperative seizure freedom, which leverages both magnetoencephalography and intracranial EEG recordings, could aid patient counselling of expected outcome.

- 1 CNRP Lab, Interdisciplinary Computing and Complex BioSystems Group, School of Computing, Newcastle University, Newcastle upon Tyne NE4 5TG, UK
- 2 UCL Queen Square Institute of Neurology, London WC1N 3BG, UK
- 3 National Hospital for Neurology & Neurosurgery, London WC1N 3BG, UK
- 4 NIHR University College London Hospitals Biomedical Research Centre, UCL Queen Square Institute of Neurology, London WC1N 3BG, UK
- 5 Faculty of Medical Sciences, Newcastle University, Newcastle upon Tyne NE1 7RU, UK

Received April 11, 2023. Revised August 24, 2023. Accepted October 24, 2023. Advance access publication October 25, 2023

© The Author(s) 2023. Published by Oxford University Press on behalf of the Guarantors of Brain.

This is an Open Access article distributed under the terms of the Creative Commons Attribution License (<https://creativecommons.org/licenses/by/4.0/>), which permits unrestricted reuse, distribution, and reproduction in any medium, provided the original work is properly cited.

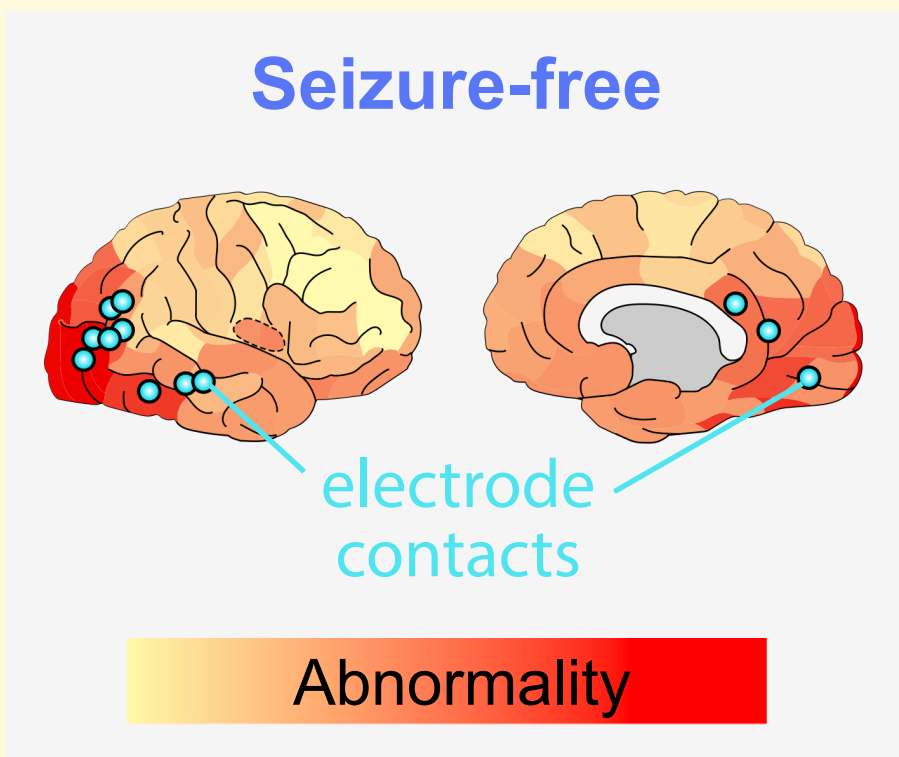
Correspondence to: Peter N. Taylor

CNNP Lab, Interdisciplinary Computing and Complex BioSystems Group, School of Computing, Newcastle Helix, Newcastle University, Newcastle upon Tyne NE4 5TG, UK

E-mail: peter.taylor@newcastle.ac.uk

Keywords: MEG; iEEG; normative; epilepsy; surgery

Graphical Abstract



Introduction

Intracranial EEG (iEEG) recordings are widely considered as the gold standard technique to accurately localize the epileptogenic zone (EZ—the part of the brain indispensable for seizures). Multiple markers of the EZ have been developed from interictal spikes¹⁻⁴ and high-frequency oscillations,⁵⁻¹² to the ictal onset patterns themselves.¹³ Successful iEEG implantation requires a preconceived hypotheses of the location of epileptogenic tissue. Thus, if the EZ is not sampled by electrodes, one may expect poorer post-surgical outcomes.

The planning of iEEG electrodes depends on seizure semiology, MRI, scalp EEG and magnetoencephalography (MEG). MEG recordings may aid electrode implantation; however, most analyses largely remain qualitative and mainly investigating spikes.¹⁴⁻¹⁹ Band power abnormality maps from interictal MEG data recently quantified epileptogenic tissue in individuals with refractory neocortical epilepsy using a data-driven framework and demonstrated localization overlap with subsequent resection in seizure-free patients and limited

overlap in those with poor surgical outcomes.²⁰ With complete cortical coverage, and sensitivity to abnormalities, MEG band power abnormality maps may be of use to localize the EZ and guide intracranial electrode placement.

Although both modalities capture neurophysiological activity, iEEG and MEG are differentially sensitive to sources of activity and thus provide complementary information. As pyramidal cells are organized perpendicular to the cortex, iEEG typically reflects extracellular sources whilst MEG reflects intracellular sources.²¹ As such, iEEG and MEG are more sensitive to sources located at the crowns of gyri, and sulci and fissures, respectively, depending on placement.²² Likewise, scalp EEG is an alternative non-invasive modality which may provide additional complementary information to MEG and iEEG, with previous studies reporting an overlap in normative maps²³ and similarities between the localization of interictal epileptiform discharges and the ground-truth irritative zone.²⁴ It is possible that multimodal abnormality mapping may provide a more complete view of the epileptogenic zone and thus further aid clinical decision-making.

In this study, we performed a multimodal analysis to investigate two primary hypotheses. First, we quantified if intracranial electrodes were implanted in regions of high MEG abnormality and hypothesized a greater overlap in patients who were seizure-free after resection. Second, we hypothesized that if electrodes were implanted in regions of high abnormality, then seizure freedom would be expected if the greatest abnormalities in both modalities were also resected.

Methods

Patient and control data

We retrospectively analysed data from 32 individuals with refractory neocortical epilepsy who underwent resective surgery. Surgical success was defined using the International League Against Epilepsy (ILAE) scoring²⁵ 1 year postoperatively. Twelve individuals were entirely seizure-free after surgical intervention (ILAE 1). No significant differences were present between surgical outcome groups based on age, sex and epilepsy duration (Table 1). All individuals underwent preoperative MEG and then subsequent intracranial EEG recordings as part of their presurgical evaluation. MEG data in the form of spike dipole clustering were available to the surgical team during the implantation of intracranial electrodes; however, the MEG measures used throughout this manuscript were derived retrospectively and so were not used to guide implantation. Additionally, T₁-weighted MRI scans were acquired for each individual both pre- and postoperatively. For normative baselines, 70 healthy controls underwent eyes-closed resting-state MEG recordings in Cardiff²⁶ and 234 individuals underwent invasive intracranial recording as part of the RAM data set.

MRI preprocessing

Pre- and postoperative MRI scans were acquired for each subject with refractory epilepsy and were used to delineate their resections. In short, MRI scans were acquired using a 3 T GE Signa HDx scanner using standard imaging gradients, a maximum strength of 40 mT m^{-1} and slew rate of

150 T $m^{-1}s^{-1}$. Data were acquired using a body coil for transmission and an eight-channel phased array coil for reception. Standard clinical sequences were performed including a coronal T₁-weighted volumetric acquisition with 170 contiguous 1.1-mm-thick slices (matrix, 256 × 256; in-plane resolution, 0.9375 × 0.9375 mm). Individual MRI scans were preprocessed using FreeSurfer's pipeline 'recon-all'²⁷ and subsequently parcellated into 114 neocortical regions of interest (ROI) based on the Lausanne parcellation scheme.²⁸ To delineate the resection cavity, pre- and postoperative MRI scans were linearly coregistered using FSL and overlaid.²⁹⁻³¹ Resection volumes were manually drawn for each individual using FSLview, and pre- and postoperative volumes were estimated using custom MATLAB code.³² A region was defined as resected if the pre- and postoperative volume change exceeded 10%.²⁰ Healthy individuals at Cardiff also underwent T₁-weighted MRI acquisition using a 3 T GE Signa HDx scanner. A full description of the acquisition protocol has been described previously.²⁶

MEG processing and abnormality mapping

MEG recordings for patients and healthy control cohorts were acquired using a 275-channel CTF whole-head MEG system at different sites. Resting-state eyes-closed interictal recordings for subjects with epilepsy were acquired at UCL in London and for healthy control data at CUBRIC Cardiff as part of the MEG UK partnership. MEG recordings from both cohorts were processed in Brainstorm using previously described methods.²⁰ MEG sensor locations were coregistered to the individuals' MRI scan using fiducial points. Coregistration was performed using the three fiducial points, with manual review to determine satisfactory coregistration. Following coregistration, MEG recordings were downsampled to 600 Hz and cleaned of any artefacts. Powerline artefacts were removed between 47.5 and 52.5 Hz using a notch filter, and ocular and cardiac artefacts were removed manually using independent component analysis (ICA). Once cleaned of any artefactual noise, MEG recordings were source reconstructed using the minimum-norm imaging technique, sLORETA,³³ and an overlapping spheres headmodel. Subsequent source space time-series were downsampled into cortical regions of interest (ROIs) using the Lausanne parcellation scheme.²⁸ Finally, 70 s epochs of recordings clear of residual artefacts for each individual were used to construct neocortical maps of band power abnormalities.

To construct normative maps, regional power spectral densities were computed using Welch's method using a 2 s sliding window with 1 s overlap. Regional relative band power estimates for delta (1–4 Hz), theta (4–8 Hz), alpha (8–13 Hz), beta (13–30 Hz) and gamma (30–80 Hz, excluding 47.5–52.5 Hz) were averaged across all 70 healthy controls (Fig. 1B). Individual band power abnormality maps were derived for each region by computing the absolute Z-score relative to normative baselines for each of the five frequency bands. To reduce the dimensionality of the data,

Table 1 Summary of clinical demographics by surgical outcome groups

	Seizure-free (ILAE 1)	Non-seizure-free (ILAE 2+)	Significance
N	12	20	
Age (years)	30.5 (7.0)	32.3 (11.3)	<i>P</i> = 0.636
Sex (female/ male)	3/9	10/10	0.895
Epilepsy duration	20.5 (8.2)	20.0 (8.8)	<i>P</i> = 0.861

The mean and standard deviations are reported, mean (SD), for seizure-free (ILAE 1) and non-seizure-free (ILAE 2+) individuals. Statistical tests were performed to assess whether any differences exist between the groups. For continuous variables, two-tailed t-tests were used. For categorical features, two-tailed Chi-squared tests were used.

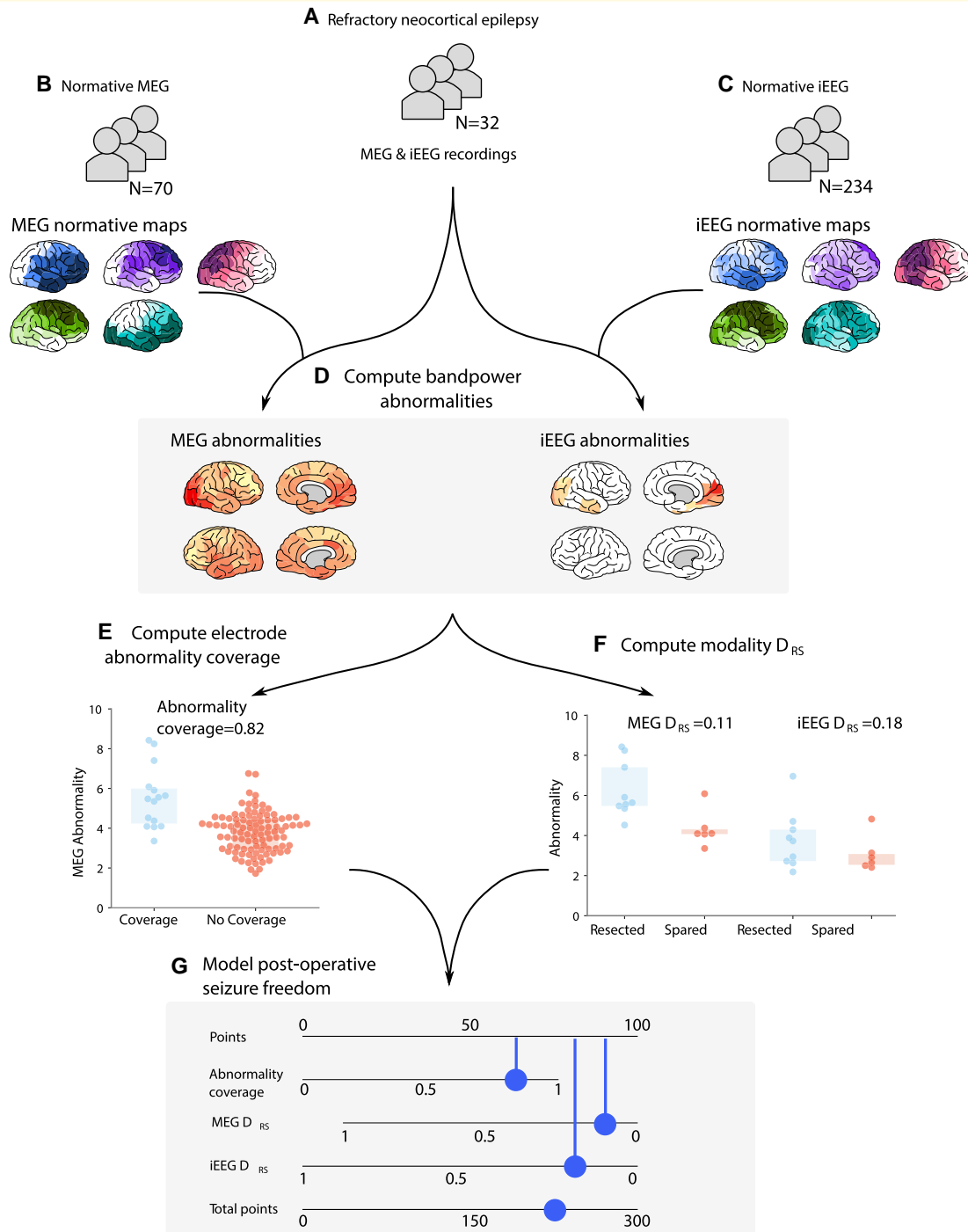


Figure 1 Processing pipeline to assess the clinical utility of MEG band power abnormalities to guide iEEG implantation. (A–C) MEG and iEEG recordings were collected for healthy and patient cohorts. Recordings for 70 healthy controls and 234 individuals with epilepsy were used as a normative baseline for MEG and iEEG, respectively. MEG and iEEG recordings were collected for an independent cohort of 32 individuals with refractory neocortical epilepsy. Regional relative band power was averaged across individuals and frequency bands to create normative maps. Patient maps of band power were derived using normative data as baselines by retaining the maximum absolute Z-score across frequencies within each region (D). The overlap between the strongest MEG abnormalities and electrode placement was quantified, defined as the abnormality coverage, with values closer to 1 corresponding to the implantation in the most abnormal tissue (E). The resection of the strongest abnormalities defined by MEG and iEEG was quantified using the distinguishability between resected and spared tissue (D_{RS}) (F). D_{RS} values closer to 0 correspond to the resection of the strongest abnormalities. The D_{RS} was only computed using neocortical tissue with MEG and iEEG coverage. The abnormality coverage and D_{RS} values per individual were used to classify postoperative seizure freedom using a logistic regression model. Model output is visualized using a nomogram (G), with each measure accruing points depending on the feature weight. The more points a subject accrues, the more likely they are to be classified as seizure-free.

we retain the maximum regional absolute Z-score across frequency bands (Fig. 1D).

iEEG processing and abnormality mapping

Long-term iEEG recordings were acquired for each individual prior to resective surgery. A cohort of 234 subjects acquired as part of the RAM data set was used to construct the normative map, using contact recordings from outside of the seizure onset and propagation zone. The RAM and UCLH data contained a mixture of subdural and depth recording data. Seventy second epochs of resting-state wakeful recordings were chosen for each individual. Similar to MEG (Section 2.3), relative band power contributions for each contact were computed for delta (1–4 Hz), theta (4–8 Hz), alpha (8–13 Hz), beta (13–30 Hz) and gamma (30–80 Hz excluding 47.5–52.5 Hz and 57.5–62.5 Hz). Note that artefacts were removed to account for interference from both US and UK powerlines (Fig. 1C).

Intracranial electrodes were localized to ROIs using standard procedures.³⁴ In short, electrodes used to construct the normative map were converted from the Talairach coordinate system to standard MNI space and assigned to an ROI in the Lausanne parcellation based on the minimum Euclidean distance. For the patient cohort, electrode assignment was performed in native space using preoperative CT and MRI scans.³⁵ For iEEG, resected tissue was defined as resected if more than 25% of the contacts within a region were resected.³⁴

Overlap between MEG abnormalities and electrode placement

We hypothesized that intracranial electrodes were implanted in regions with the greatest MEG abnormality in individuals who were seizure-free postoperatively. To quantify the degree of overlap between MEG abnormalities and intracranial electrode placement, we used the abnormality coverage. Similar to the D_{RS} ,³⁵ the abnormality coverage quantifies the degree in which electrodes are placed in tissue of strongest MEG abnormality using the area under the receiver operating characteristic (ROC) curve (AUC). Ranging between zero and one, an abnormality coverage of 1 corresponds to electrodes implanted exclusively in the most abnormal neocortical tissue. Conversely, an abnormality coverage of 0 corresponds to the electrode implantation targeting the least abnormal neocortical tissue. An abnormality coverage of 0.5 corresponds to chance and reflects the targeting of both abnormal and seemingly healthy tissue (Fig. 1E).

Overlap between neurophysiological abnormalities and resection masks

To assess whether the locations with greatest abnormalities were resected, we used the D_{RS} ^{20,34} Like the abnormality

coverage, the D_{RS} ranges from zero to one, with values of zero corresponding to the resection of the most abnormal tissue. The D_{RS} was computed for each individual using MEG and iEEG data separately using only tissue where there was MEG and electrode coverage, i.e. discarding neocortical tissue in MEG where electrodes were not implanted (Fig. 1F).

Modelling of postoperative seizure freedom

We investigated the extent to which the abnormality coverage and two D_{RS} measures explain surgical outcome using a logistic regression model. No standardization in the form of mean centring and scaling was performed prior to model fitting as all three features have natural interpretations and similar values ranges. Class weights were introduced to the model in order to account for the imbalance in surgical outcome groups (12 ILAE 1 and 20 ILAE 2+). Setting a class weight of $\frac{20}{32}$ and $\frac{12}{32}$ for seizure-free and non-seizure-free groups, respectively, penalizes the most frequent surgical outcome group (ILAE 2+) in such a way that both groups are treated equally. We report the output of the model using a nomogram (Fig. 1G). In the context of epilepsy, nomograms have previously been proposed to aid clinicians determine post-surgical seizure freedom^{36,37} and cognitive decline.^{38,39} Nomograms are commonly used as a visual representation of the Cox proportional hazard model used in survival analysis; however, they can also be used for a logistic regression model. For a given subject, each feature within the nomogram accrues points towards a final score. The number of points attributed to each feature is directly proportional to the feature importance estimated from the logistic regression model. Once all of the points for a given subject are totalled, a prediction of surgical outcome can be made based on whether the patient exceeds a given threshold determined during model training. For the nomogram presented in this study, the more points a subject accrues, the greater the confidence that they will be seizure-free postoperatively.

To assess the robustness of the predictive model to outliers in the data, we used leave-one-out validation. During leave-one-out validation, a single subject is removed from the data set, the model is recomputed, and the AUC is estimated. Once complete, the AUC scores are then averaged to obtain a robust measure of the separability of surgical outcome groups.

Statistical analysis

Statistical tests were used to assess whether the abnormality coverage and D_{RS} scores differ significantly from chance. We used a one-tailed *t*-test to check whether the abnormality coverage of seizure-free patients was significantly >0.5 . A one-tailed Mann–Whitney U test was used to quantify whether our measures significantly separated surgical outcome groups. One-tailed tests were used as clear hypotheses of direction are provided.

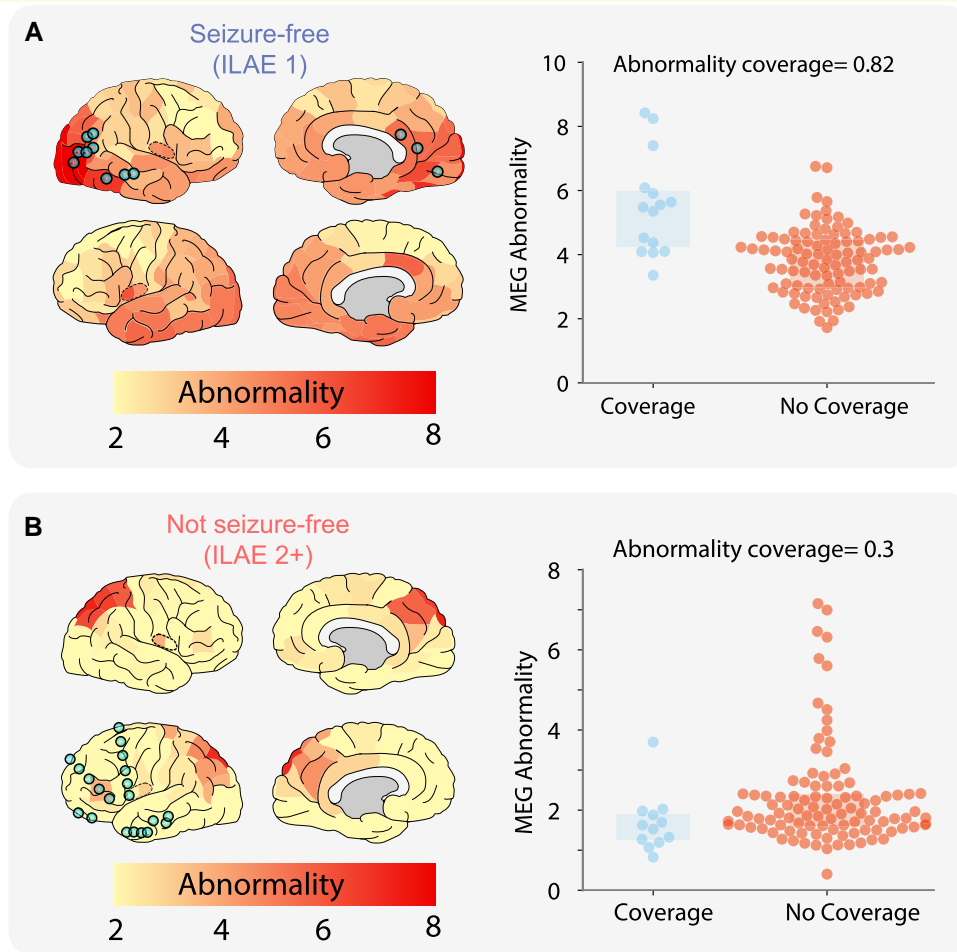


Figure 2 Overlapping MEG band power abnormalities and intracranial EEG electrode implantation. Neocortical interictal resting-state MEG band power abnormalities and iEEG electrode implantation in an example seizure-free patient (**A**). High overlap is present between MEG-derived abnormalities and iEEG electrode placement, quantified with an abnormality coverage of 0.82. In this scenario, we would expect postoperative seizure freedom as iEEG electrodes have targeted abnormal tissue presumed to contain the epileptogenic zone. (**B**) Conversely, this example subject with poor surgical outcome (ILAE 2+) has minimal overlap between MEG abnormalities and electrode placement (abnormality coverage = 0.3). As such, we would expect poor surgical outcome as the presumed epileptogenic tissue was not targeted by intracranial electrodes for further monitoring. Spatial heatmaps correspond to MEG-derived band power abnormalities, with blue points corresponding to the approximate localization of iEEG electrodes. Boxplots (right panels) illustrate the abnormality of regions with and without iEEG coverage (blue and orange, respectively). Each data point corresponds to a single neocortical region of interest. The abnormality coverage (0.82 for patient **A**) reflects if the most abnormal regions had iEEG coverage. Values closer to 1 correspond to implantation exclusively in the most abnormal tissue and values of 0 to an implantation exclusively in the least abnormal tissue.

Results

MEG abnormalities overlap with electrode placement in seizure-free patients

We investigated whether intracranial EEG electrodes were implanted in areas of strongest MEG abnormality using the ‘abnormality coverage’ metric. Two example subjects are shown in Fig. 2 with different surgical outcomes. In the seizure-free patient (Fig. 2A), a strong overlap exists between the iEEG electrode implantation and strongest MEG

abnormalities. This is quantified with an abnormality coverage score of 0.82, signifying that electrodes were indeed implanted in the most abnormal neocortical tissue, as defined by resting-state interictal MEG band power.

In contrast to the seizure-free individual, Fig. 2B illustrates the overlap between iEEG electrodes and MEG abnormalities for a non-seizure-free subject. It is clear that electrode implantation does not overlap well with the MEG-derived abnormalities, with the strongest abnormalities located in the right occipital and parietal tissue and electrodes implanted in the left frontal tissue. The minimal overlap between iEEG electrode placement and MEG band power

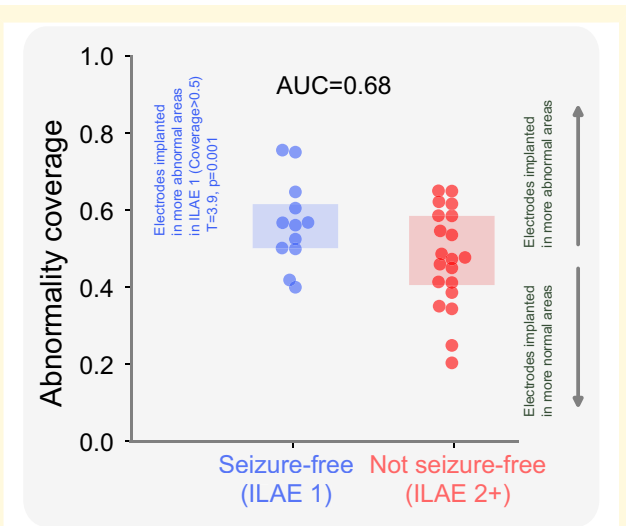


Figure 3 Surgical outcome separability of the abnormality coverage at a group level. The boxplot shows the abnormality coverage measure for seizure-free (ILAE 1) and non-seizure-free subjects (ILAE 2+). Each data point corresponds to an individual subject. Seizure-free subjects are significantly >0.5 indicating coverage in regions with high MEG abnormality ($T=3.9$, $P=0.001$). This effect was not present for ILAE 2+ patients. Differences between each group of individuals relative to 0.5 were estimated using a one-tailed one sample *t*-test. One-tailed tests were used as clear preconceived hypotheses were provided. AUC = area under the receiver operating characteristic curve.

abnormalities is captured by the abnormality coverage measure with a value of 0.3.

We expanded our analysis to the full cohort of 32 individuals, reporting the overlap between electrode placement and MEG abnormalities (Fig. 3). Individuals who were seizure-free postoperatively had greater overlap between MEG band power abnormalities and electrode placement, characterized by larger abnormality coverage values, than non-seizure-free individuals. The implantation of electrodes in tissue of strongest MEG abnormality occurred in seizure-free patients (ILAE 1) greater than chance ($T=3.9$, $P=0.001$). The effect of electrodes overlapping with MEG abnormalities separates surgical outcome groups well (AUC = 0.68).

Taken together, these results suggest that patients had better outcomes if their MEG-derived abnormalities were sampled by intracranial EEG.

Multimodal abnormality maps predict postoperative seizure freedom

We next investigated if the strongest MEG and iEEG abnormalities were resected. To quantify this, we used the D_{RS} metric, considering only tissue which had MEG and iEEG coverage (Supplementary Fig. 1). In agreement with our prior studies,^{20,34} the resection of the strongest

abnormalities was typically observed in seizure-free patients. The effect separating surgical outcome groups well for both MEG, AUC = 0.71, and iEEG, AUC = 0.74. Subject data and measures are reported in Supplementary Table 1.

We hypothesized that the combination of abnormality coverage and two D_{RS} measures would explain surgical outcome best. Our rationale was that D_{RS} would perform best for seizure-free patients only if abnormalities were actually covered, hence the inclusion of all three metrics. To combine measures, we used a logistic regression model and report the output as a nomogram (Fig. 4A). All three measures contributed towards the prediction of postoperative seizure freedom. The implantation of electrodes in MEG-defined abnormal regions, and subsequent concordance between MEG and iEEG, separated outcome groups best (Fig. 4B). Robust measures of model performance using a leave-one-out approach resulted in an average AUC of 0.79 (min = 0.77, max = 0.84). We replicated our analysis using different thresholds to define resected tissue (Supplementary Fig. 2). The findings were broadly consistent across a range of thresholds for resection.

Together, the results of this study suggest that resting-state interictal MEG band power abnormality mapping may provide localizing information which can be leveraged for electrode implantation. Furthermore, we show that a multimodal model (incorporating both iEEG and MEG) offers clinically interpretable predictions which may be of value during the presurgical evaluation.

Discussion

Accurate delineation and resection of epileptogenic tissue is key to achieve postoperative seizure freedom.⁴⁰ Intracranial EEG is widely used to delineate the EZ in difficult to localize individuals. Hypotheses of epileptogenic tissue location are required in order to guide electrode implantation. In this study, we demonstrated that data-driven measures of neocortical abnormality using interictal MEG band power are associated with electrode implantation strategies in successful surgery candidates. Moreover, we showed that a multimodal model of post-surgical seizure freedom outperforms any measure in isolation. Together, our results suggest that MEG band power abnormality mapping may complement current iEEG implantation strategies, providing clinically useful information to aid decision-making during the presurgical evaluation.

Intracranial EEG recordings are used if the mapping of epileptogenic tissue using non-invasive modalities are inconclusive, discordant and uncertain of epileptogenic network involvement or indicate a close proximity to eloquent tissue.⁴¹⁻⁴³ To minimize the risks attributed with iEEG⁴⁴ and maximize its effectiveness, a clear hypothesis of the EZ is required in order to guide electrode implantation. At present, implantation strategies are determined by clinical teams, usually based on visual evaluation of non-invasive modalities and seizure semiologies. Our MEG-derived spatial maps of

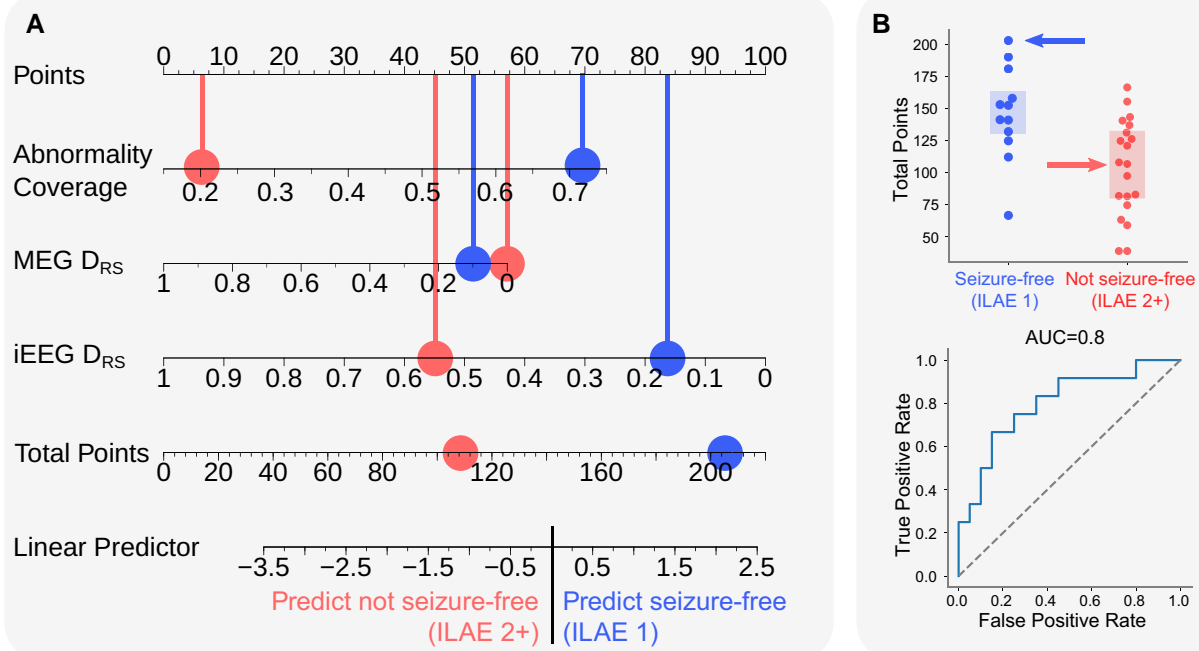


Figure 4 Modelling post-surgical seizure freedom using multimodal measures. (A) Nomogram illustrating the output of a logistic regression model trained using the abnormality coverage, MEG D_{RS} and iEEG D_{RS} . Here, D_{RS} represents the distinguishability between resected and spared tissue in the respective modality. Each feature accrues points towards a final score. The points for an individual subject based on their measures are totalled and subsequently compared across surgical outcome groups. Each blue point corresponds to the results for a single seizure-free patient, whereas red points correspond to the results for a single non-seizure-free subject. We hypothesized that the more points a subject accrued, the more likely they would be seizure-free postoperatively as the abnormality coverage indicates that potentially epileptogenic tissue had been targeted for iEEG monitoring and that MEG and iEEG are in agreement that most abnormal tissue was resected. (B) For each individual, the total points calculated using the nomogram were compared across surgical outcome groups. The model results are presented as a boxplot and ROC curve. Each point corresponds to a single individual (ILAE 1, blue; ILAE 2+, red). The significance of our result was quantified using an AUC score derived from a one-tailed Mann–Whitney U test (AUC = 0.8, $P = 0.003$). A one-tailed test was performed as a clear hypothesis of direction was provided.

band power abnormalities indicate a stronger overlap between the most abnormal tissue and the implantation of iEEG electrodes in seizure-free subjects (Fig. 3). As such, our data-driven abnormality maps may complement current strategies by validating the proposed electrode implantation or by directing implantation to other brain areas.

Several studies have proposed the use of MEG recordings to help inform iEEG electrode placement.^{14–19,45,46} Magnetic source imaging (MSI) indicated additional electrode coverage beyond the initially proposed hypothesis of epileptogenic tissue in 23% of subjects.¹⁶ Moreover, in 39% of subjects, the authors report seizure onset activity in the electrodes proposed by MSI. Frequent and densely clustered interictal MEG spikes were correlated with iEEG placement in 69% of subjects in whom the seizure onset zone was localized.²⁶ Our study builds on this literature, using a data-driven framework to relate interictal MEG band power abnormalities to iEEG electrode placement without the need to mark interictal spikes.

Interictal markers of the epileptogenic zone have been developed using high-frequency oscillations (HFOs),^{7,9,10,47,48} spikes^{3,4,49} and networks.^{50–57} Moreover, the use of electric

source imaging has shown promise in the localization of the EZ.^{58,59} In this study, we focus on the mapping of interictal band power abnormalities. Recent studies have demonstrated that the resection of the strongest abnormalities defined by iEEG^{34,60} and MEG²⁰ in isolation is associated with post-surgical seizure freedom. As MEG and iEEG recordings are sensitive to different types of sources,^{21,22} we investigated whether concordant markers of epileptogenic tissue derived from the same individuals using MEG and iEEG yielded a better resolution for the delineation of epileptogenic tissue.

Our model of postoperative seizure freedom follows an intuitive thought process. First, MEG abnormalities must be investigated by intracranial EEG electrodes. Second, those regions must also be abnormal using iEEG. Third, those abnormal regions must be resected. If those three criteria are met, then the chance of seizure freedom is extremely high. We presented our model of three properties using a nomogram, a visual tool used to illustrate complex multivariable linear models. Recent studies have proposed the use of nomograms in the context of epilepsy to aid prediction of postoperative seizure freedom^{36,37} and cognitive decline.^{38,39}

Our multimodal model of post-surgical seizure freedom outperforms our single measures in isolation (AUC =0.8). Interestingly, the feature weights of the model were roughly similar (Fig. 4A), suggesting all three contribute to the best predictions of outcome. Our results indicate that MEG and iEEG band power abnormalities contain complementary information which may aid clinical decision-making during the presurgical evaluation.

This study has several strengths and limitations. One strength is the data-driven nature of MEG and iEEG band power abnormalities, negating the need for manual spike marking, which can be prone to human bias.⁶¹ Band power mapping however is relatively invariant to changes in spike rate and magnitude and offers different information.³⁴ The overlap of interictal biomarkers such as spikes and HFOs has shown promise as a marker of the epileptogenic zone.^{24,62} For example, the resection of interictal spikes has been shown to relate to surgical outcome.^{1,4} Future work investigating the relationship between our band power abnormalities and other makers of epileptogenic tissue could yield further discriminatory power and benefit studies where only recordings from a single modality are available. A key limitation of this study is the sample size, though to our knowledge, it is still one of the largest quantitative studies of iEEG and MEG with gold standard post-operative MRI for resection delineation. Nonetheless, future studies using larger cohorts could validate the techniques proposed. Moreover, the difficulty in localizing weak signals in subcortical structures precludes the accurate analysis of individuals with seizures of temporal origin. The addition of abnormality maps derived using structural modalities such as T₁-weighted MRI or diffusion MRI may circumvent the current limitation of limited coverage in deep brain structures.⁶³

Markers of epileptogenic tissue derived using iEEG have consistently been shown to relate to surgical outcome. Yet, iEEG implantation requires preconceived ideas of the location of epileptogenic tissue, usually acquired using qualitative techniques. We proposed interictal MEG band power abnormality mapping as a data-driven approach to complement current iEEG implantation strategies. Our findings further highlight the clinical value of MEG band power abnormalities for individuals with drug refractory neocortical epilepsy.

Supplementary material

Supplementary material is available at *Brain Communications* online.

Acknowledgements

We thank members of the Computational Neurology, Neuroscience & Psychiatry Lab (www.cnnp-lab.com), for discussions on the analysis and manuscript.

Funding

The normative data collection was supported by a Medical Research Council UK Partnership Grant (MR/K005464/1). T.W.O. is supported by the Centre for Doctoral Training in Cloud Computing for Big Data (EP/L015358/1). P.N.T. and Y.W. are both supported by UK Research & Innovation Future Leaders Fellowships (MR/T04294X/1 and MR/V026569/1). B.D. receives support from the National Institutes of Health National Institute of Neurological Disorders and Stroke (U01-NS090407) (Center for Sudden Unexpected Death in Epilepsy Research) and Epilepsy Research UK. J.S.D is supported by the Wellcome Trust grant 218380. J.S.D and J.d.T. are supported by the National Institute for Health Research University College London Hospitals Biomedical Research Centre, UCL Queen Square Institute of Neurology, London WC1N 3BG, UK.

Competing interests

The authors report no competing interests.

Data availability

Data and code to reproduce the main findings of the study are available at the following location: https://github.com/cnnp-lab/Using_MEG_abnormalities_to_guide_intracranial_electrode_implantation.

References

1. Kim DW, Kim HK, Lee SK, Chu K, Chung CK. Extent of neocortical resection and surgical outcome of epilepsy: Intracranial EEG analysis. *Epilepsia* 2010;51(6):1010-1017.
2. Megevand P, Spinelli L, Genetti M, et al. Electric source imaging of interictal activity accurately localises the seizure onset zone. *J Neurol Neurosurg Psychiatry*. 2014;85(1):38-43.
3. Kim DW, Lee SK, Moon HJ, Jung KY, Chu K, Chung CK. Surgical treatment of nonlesional neocortical epilepsy: Long-term longitudinal study. *JAMA Neurol*. 2017;74(3):324-331.
4. Azeem A, von Ellenrieder N, Hall J, Dubeau F, Frauscher B, Gotman J. Interictal spike networks predict surgical outcome in patients with drug-resistant focal epilepsy. *Ann Clin Transl Neurol*. 2021;8(6):1212-1223.
5. Foley E, Quitadamo LR, Walsh AR, Bill P, Hillebrand A, Seri S. MEG detection of high frequency oscillations and intracranial-EEG validation in pediatric epilepsy surgery. *Clin Neurophysiol*. 2021;132(9):2136-2145.
6. van Klink N, Hillebrand A, Zijlmans M. Identification of epileptic high frequency oscillations in the time domain by using MEG beamformer-based virtual sensors. *Clin Neurophysiol*. 2016;127(1):197-208.
7. Jacobs J, Zijlmans M, Zelman R, et al. High-frequency electroencephalographic oscillations correlate with outcome of epilepsy surgery. *Ann Neurol*. 2010;67(2):209-220.
8. van Klink NEC, van't Klooster MA, Zelman R, et al. High frequency oscillations in intra-operative electrocorticography before

- and after epilepsy surgery. *Clin Neurophysiol.* 2014;125(11):2212-2219.
9. Fujiwara H, Leach JL, Greiner HM, *et al.* Resection of ictal high frequency oscillations is associated with favorable surgical outcome in pediatric drug resistant epilepsy secondary to tuberous sclerosis complex. *Epilepsy Res.* 2016;126:90-97.
 10. Fedele T, Burnos S, Boran E, *et al.* Resection of high frequency oscillations predicts seizure outcome in the individual patient. *Sci Rep.* 2017;7(1):13836.
 11. Nevalainen P, von Ellenrieder N, Klimesš P, Dubeau F, Frauscher B, Gotman J. Association of fast ripples on intracranial EEG and outcomes after epilepsy surgery. *Neurology* 2020;95(16):e2235-e2245.
 12. Nunez MD, Charupanit K, Sen-Gupta I, Lopour BA, Lin JJ. Beyond rates: Time-varying dynamics of high frequency oscillations as a biomarker of the seizure onset zone. *J Neural Eng.* 2022;19(1):016034.
 13. Lagarde S, Buzori S, Trebuchon A, *et al.* The repertoire of seizure onset patterns in human focal epilepsies: Determinants and prognostic values. *Epilepsia* 2019;60(1):85-95.
 14. Mamelak AN, Lopez N, Akhtari M, Sutherling WW. Magnetoencephalography-directed surgery in patients with neocortical epilepsy. *J Neurosurg.* 2002;97(4):865-873.
 15. Sutherling WW, Mamelak AN, Thyerlei D, *et al.* Influence of magnetic source imaging for planning intracranial EEG in epilepsy. *Neurology* 2008;71(13):990-996.
 16. Knowlton RC, Razdan SN, Limdi N, *et al.* Effect of epilepsy magnetic source imaging on intracranial electrode placement. *Ann Neurol.* 2009;65(6):716-723.
 17. Vitikainen A-M, Lioumis P, Paetau R, *et al.* Combined use of non-invasive techniques for improved functional localization for a selected group of epilepsy surgery candidates. *NeuroImage* 2009;45(2):342-348.
 18. Agirre-Arribieta Z, Thai NJ, Valentín A, *et al.* The value of magnetoencephalography to guide electrode implantation in epilepsy. *Brain Topogr.* 2014;27(1):197-207.
 19. Anand A, Magnotti JF, Smith DN, *et al.* Predictive value of magnetoencephalography in guiding the intracranial implant strategy for intractable epilepsy. *J Neurosurg.* 2022;137(5):1237-1247.
 20. Owen TW, Schroeder GM, Janiukstyte V, *et al.* MEG abnormalities and mechanisms of surgical failure in neocortical epilepsy. *Epilepsia* 2023;64(3):692-704.
 21. Lopes da Silva F. EEG and MEG: Relevance to neuroscience. *Neuron* 2013;80(5):1112-1128.
 22. Hansen PC, Kringelbach ML, Salmelin R, eds. *MEG: An Introduction to methods.* Oxford University Press; 2010:1-423.
 23. Janiukstyte V, Owen TW, Chaudhary UJ, *et al.* Normative brain mapping using scalp EEG and potential clinical application. *Sci Rep.* 2023;13(1).
 24. Tamilya E, Dirodi M, Alhilani M, *et al.* Scalp ripples as prognostic biomarkers of epileptogenicity in pediatric surgery. *Ann Clin Transl Neurol.* 2020;7(3):329-342.
 25. Wieser HG, Blume WT, Fish D, *et al.* Proposal for a new classification of outcome with respect to epileptic seizures following epilepsy surgery. *Epilepsia* 2001;42(2):282-286.
 26. Messaritari E, Foley S, Schiavi S, *et al.* Predicting MEG resting-state functional connectivity from microstructural information. *Network Neurosci.* Published online April 2021;5(2):477-4504.
 27. Fischl B. FreeSurfer. *NeuroImage* 2012;62(2):774-781.
 28. Hagmann P, Cammoun L, Gigandet X, *et al.* Mapping the structural core of human cerebral cortex. *PLoS Biol.* 2008;6(7):e159.
 29. Jenkinson M, Bannister P, Brady M, Smith S. Improved optimization for the robust and accurate linear registration and motion correction of brain images. *NeuroImage* 2002;17(2):825-841.
 30. Jenkinson M, Beckmann CF, Behrens TEJ, Woolrich MW, Smith SM. FSL. *NeuroImage* 2012;62(2):782-790.
 31. Greve DN, Fischl B. Accurate and robust brain image alignment using boundary-based registration. *NeuroImage* 2009;48(1):63-72.
 32. Taylor PN, Sinha N, Wang Y, *et al.* The impact of epilepsy surgery on the structural connectome and its relation to outcome. *NeuroImage Clin.* 2018;18:202-214.
 33. Tenney JR, Fujiwara H, Rose DF. The value of source localization for clinical magnetoencephalography: Beyond the equivalent current dipole. *J Clin Neurophysiol.* 2020;37(6):537-544.
 34. Taylor PN, Papanavvas CA, Owen TW, *et al.* Normative brain mapping of interictal intracranial EEG to localize epileptogenic tissue. *Brain* Published online January 2022;145(3):949.
 35. Wang Y, Sinha N, Schroeder GM, *et al.* Interictal intracranial electroencephalography for predicting surgical success: The importance of space and time. *Epilepsia* 2020;61(7):1417-1426.
 36. Jehi L, Yardi R, Chagin K, *et al.* Development and validation of nomograms to provide individualised predictions of seizure outcomes after epilepsy surgery: A retrospective analysis. *Lancet Neurol.* 2015;14(3):283-290.
 37. Morita-Sherman M, Li M, Joseph B, *et al.* Incorporation of quantitative MRI in a model to predict temporal lobe epilepsy surgery outcome. *Brain Commun.* 2021;3(3):fcb164.
 38. Busch RM, Hogue O, Kattan MW, *et al.* Nomograms to predict naming decline after temporal lobe surgery in adults with epilepsy. *Neurology* 2018;91(23):e2144-e2152.
 39. Busch RM, Hogue O, Miller M, *et al.* Nomograms to predict verbal memory decline after temporal lobe resection in adults with epilepsy. *Neurology* 2021;97(3):e263-e274.
 40. Rosenow F, Lüders H. Presurgical evaluation of epilepsy. *Brain* 2001;124(9):1683-1700.
 41. Shah AK, Mittal S. Invasive electroencephalography monitoring: Indications and presurgical planning. *Ann Indian Acad Neurol.* 2014;17(Suppl 1):S89-S94.
 42. Kovac S, Vakharia VN, Scott C, Diehl B. Invasive epilepsy surgery evaluation. *Seizure* 2017;44:125-136.
 43. Duncan JS. Multidisciplinary team meetings: The epilepsy experience. *Pract Neurol.* 2022;22(5):376-380.
 44. Meng Y, Voisin MR, Suppiah S, *et al.* Risk factors for surgical site infection after intracranial electroencephalography monitoring for epilepsy in the pediatric population. *J Neurosurg Pediatr.* 2018;22(1):31-36.
 45. Corona L, Tamilya E, Madsen JR, Stufflebeam SM, Pearl PL, Papadelis C. Mapping functional connectivity of epileptogenic networks through virtual implantation. *2021 43rd Ann Int Conf IEEE Eng Med Biol Soc (EMBC).* 2021;1:408-411.
 46. Velmurugan J, Badier JM, Pizzo F, *et al.* Virtual MEG sensors based on beamformer and independent component analysis can reconstruct epileptic activity as measured on simultaneous intracerebral recordings. *NeuroImage* 2022;264:119681.
 47. Tamilya E, Madsen JR, Grant PE, Pearl PL, Papadelis C. Current and emerging potential of magnetoencephalography in the detection and localization of high-frequency oscillations in epilepsy. *Front Neurol.* 2017;8. Accessed March 20, 2023. <https://www.frontiersin.org/articles/10.3389/fneur.2017.00014>
 48. Tamilya E, Matarrese MAG, Ntolkeras G, *et al.* Noninvasive mapping of ripple onset predicts outcome in epilepsy surgery. *Ann Neurol.* 2021;89(5):911-925.
 49. Ntolkeras G, Tamilya E, Alhilani M, *et al.* Presurgical accuracy of dipole clustering in MRI-negative pediatric patients with epilepsy: Validation against intracranial EEG and resection. *Clin Neurophysiol.* 2022;141:126-138.
 50. Englot DJ, Konrad PE, Morgan VL. Regional and global connectivity disturbances in focal epilepsy, related neurocognitive sequelae, and potential mechanistic underpinnings. *Epilepsia* 2016;57(10):1546-1557.
 51. Nissen IA, Stam CJ, Reijneveld JC, *et al.* Identifying the epileptogenic zone in interictal resting-state MEG source-space networks. *Epilepsia* 2017;58(1):137-148.
 52. Nissen IA, Stam CJ, van Straaten ECW, *et al.* Localization of the epileptogenic zone using interictal MEG and machine learning in a

- large cohort of drug-resistant epilepsy patients. *Front Neurol.* 2018;9.
53. Morgan VL, Rogers BP, González HFJ, Goodale SE, Englot DJ. Characterization of postsurgical functional connectivity changes in temporal lobe epilepsy. *J Neurosurg.* 2019;133:392-3402.
 54. Zweiphenning WJEM, Keijzer HM, van Diessen E, *et al.* Increased gamma and decreased fast ripple connections of epileptic tissue: A high-frequency directed network approach. *Epilepsia* 2019;60(9):1908-1920.
 55. Aydin Ü, Pellegrino G, Bin Ka'b Ali O, *et al.* Magnetoencephalography resting state connectivity patterns as indicatives of surgical outcome in epilepsy patients. *J Neural Eng.* Published online March 2020;17(3):035007.
 56. Ramaraju S, Wang Y, Sinha N, *et al.* Removal of interictal MEG-derived network hubs is associated with postoperative seizure freedom. *Front Neurol.* 2020;11.
 57. Corona L, Tamilia E, Perry MS, *et al.* Non-invasive mapping of epileptogenic networks predicts surgical outcome. *Brain* Published online February 2023;146(5):1916-1931.
 58. Kaiboriboon K, Lüders HO, Hamaneh M, Turnbull J, Lhatoo SD. EEG source imaging in epilepsy—practicalities and pitfalls. *Nat Rev Neurol.* 2012;8(9):498-507.
 59. Cox BC, Danoun OA, Lundstrom BN, Lagerlund TD, Wong-Kissel LC, Brinkmann BH. EEG source imaging concordance with intracranial EEG and epileptologist review in focal epilepsy. *Brain Commun.* 2021;3(4):fcab278.
 60. Bernabei JM, Sinha N, Arnold TC, *et al.* Normative intracranial EEG maps epileptogenic tissues in focal epilepsy. *Brain* Published online May 2022;145(6):1949-1961.
 61. Jing J, Sun H, Kim JA, *et al.* Development of expert-level automated detection of epileptiform discharges during electroencephalogram interpretation. *JAMA Neurol.* 2020;77(1):103-108.
 62. Cai Z, Sohrabpour A, Jiang H, *et al.* Noninvasive high-frequency oscillations riding spikes delineates epileptogenic sources. *Proc Natl Acad Sci USA.* 2021;118(17):e2011130118.
 63. Horsley JJ, Thomas RH, Chowdhury FA, *et al.* Complementary structural and functional abnormalities to localise epileptogenic tissue. *eBioMedicine.* 2023;97:104848. doi: 10.1016/j.ebiom.2023.104848.